A P P E N D I X

FLUORESCENCE DYNAMICS OF LYSOSOMAL-RELATED ORGANELLE FLASHING IN THE INTESTINAL CELLS OF *CAENORHABDITIS ELEGANS*

C. Tan., Ding, K., Anderson, D. J., Sternberg, P.W. Fluorescence dynamics of lysosomal-related organelle dissipation in the intestinal cells of *Caenorhabditis elegans* (In preparation)

Summary

Autofluorescent lysosome-related organelles (or gut granules) in the intestinal cells of *Caenorhabditis elegans* have been shown to play an important role in metabolic and signaling processes, but they have not been fully characterized. Using a preparation comprising live worms with intestinal tissue exposed, we report here a previously undescribed phenomenon in which gut granule autofluorescence is quenched in a rapid and dynamic manner. We show that at least two types of fluorophores are present in the gut granules. One displayed a "flashing" phenomenon, in which quenching is preceded by a sharp increase in fluorescence intensity that expands into the surrounding area. The flashing phenomenon is strongly correlated with food availability, suggesting that the underlying activities are likely to be physiological and may be part of a metabolic process.

Introduction

The intestinal cells of *Caenorhabditis elegans* and related nematodes are known to contain a type of organelle known as gut granules or rhabditin granules (Chitwood & Chitwood, 1950; Laufer, Bazzicalupo, & Wood, 1980). These birefringent and autofluorescent granules are robustly present in intestinal and intestinal precursor cells and thus serve as a useful marker for the intestinal linage

(Hermann et al., 2005; Laufer et al., 1980). Based on morphological, biochemical, and genetic evidence, these granules are considered to be lysosome-related organelles (Clokey & Jacobson, 1986; Hermann et al., 2005; Kostich, Fire, & Fambrough, 2000). As with lysosome-related organelles in other organisms, the biological roles of gut granules are not fully understood. There is evidence, however, that these organelles are likely to be involved in metabolic and homeostatic processes such as the storage of fat and cholesterol (Lee et al., 2015; Schroeder et al., 2007) and trace metal storage and detoxification (Chun et al., 2017; Roh, Collier, Guthrie, Robertson, & Kornfeld, 2012). In addition, gut granules are also known to play a signaling role through the biogenesis of ascarosides (Le et al., 2020).

In this study, we show that in partially exposed *C. elegans* intestinal tissue, some autofluorescent granules underwent a rapid and dynamic change in fluorescence intensity. Since the spatio-temporal pattern of the dynamic changes in green and red fluorescence channels are different, we concluded that at least two different fluorophores are present in the gut granule and were involved in this process. Prior to fluorescence dissipation, there was a sharp and significant increase in green fluorescence intensities that extended to the surrounding areas, a phenomenon that we describe as "flashing." Gut granule flashing was strongly dependent on food availability at the time of the experiments, being almost entirely absent in preparations without added food. Finally, we show that the worm ortholog of human Rab32/38, *glo-1* (Gut granule LOss) (Hermann et al., 2005; Morris et al., 2018), which has been shown to be required for gut granules biogenesis, was necessary for the flashing phenotype, suggesting that the source of the autofluorescent flashing signals was indeed gut granules. We have yet to identify the fluorophores responsible for the phenomenon, the underlying

biochemical processes or its biological significance. However, we found this to be an intriguing phenomenon providing insights into the functions and mechanisms of lysosome-related organelles.

Results

Some autofluorescent granules in intestinal cells displayed dynamic changes in fluorescent intensities

During our observational analysis of exposed *Caenorhabditis elegans* intestine with fluorescence confocal microscopy, in which the worm is cut open near the anus to expose the intestine (Fig 1B), we observed that some of the fluorescent granules in the intestinal cells displayed dynamic changes in fluorescence intensity (Fig 1A, C, S1 Movie). In these granules, the green fluorescence, illuminated with the 473nm laser of the confocal microscope, rises sharply and significantly (Fig 1A, C, D, S1 Movie). The intensity increase is not only limited to the original "core" area (the granule proper), as identified by the high level of fluorescence at a steady-state prior to the rapid intensity changes, but also to the surrounding areas (which we refer to as the "cloud." Details of how the area is identified are in the Methods; Fig 1E). The fluorescence intensity in both the "core" and the surrounding areas subsequently dropped off, with the intensity at the "core" dropping to a level that is lower than the previous steady-state, and the intensity in the surrounding areas ("clouds") decreasing to a level that is similar to the previous steady-state (Fig 1E). We estimated that the rapid changes in fluorescence intensity occur in less than 10 seconds, in a way that resembles the bursting of fireworks or the flashing of a light (Fig 1E). In contrast, the red fluorescent signal, illuminated with the 561nm laser of the confocal microscope, lacked the initial sharp increase observed within the green fluorescence channel, but fell concurrently (Fig 1F). The dynamic differences observed in the green and red fluorescent channels suggest that they may represent at least two distinct types of

fluorophores presented in the autofluorescent granules. This phenomenon is rare but is consistently observed in a portion of the animals in this preparation through over two years of study. The fluorophore is not exogenous, as the phenomena can be observed in wild-type animals, which were used exclusively in this study.

The autofluorescent granules flashing phenomena are strongly correlated with food availability

Since the primary function of the intestine is food digestion, we reasoned that the autofluorescent granules flashing phenomena could be associated with nutrient uptake. In *C. elegans*, food availability significantly influences the rhythmic defecation cycle (Thomas, 1990), which is controlled by calcium oscillations in the intestinal cells (Dal Santo, Logan, Chisholm, & Jorgensen, 1999). To test whether granule flashing phenomena are associated with food availability, we provided food (*Escherichia coli* OP50) to the experimental animal on the microscopic slides. We found that in worms with a significant amount of food near the head region, the occurrence of the granule flashing phenomena increased dramatically (Fig. 2A-D, S1 Movie). All seven worms provided with food displayed the phenomena (Fig. 2C, D, H), while only 1 of 7 without food did at a low frequency (Fig. 2A, B, H). It is worth noting that a small amount of food is still present in the "no food" group, which may explain the occasional occurrence of the phenomena.

The flashing autofluorescent granules are lysosome-related organelles

The worm intestinal cells are known to contain numerous autofluorescent granules known as "gut granules" (Hermann et al., 2005; Laufer et al., 1980). Gut granules are lysosome-related organelles that have been shown to play an important physiological role in both nutrient homeostasis and signal

transduction (Chun et al., 2017; Le et al., 2020; Roh et al., 2012; Schroeder et al., 2007). To characterize the nature of the observed autofluorescent granules flashing phenomena, we analyzed *glo-1(lf)* mutant animals that are defective in gut granules biogenesis. *glo-1* (Gut granule LOss) encodes an ortholog of Rab32/38 that localize to gut granules (Hermann et al., 2005; Morris et al., 2018). *glo-1(lf)* animals displayed a large reduction in the number of autofluorescent granules in the intestine, similar to what was described in Hermann et al. (2005), and also completely eliminated the granules flashing phenomena (Fig. 2E, F, H). Even with food provided, none of the seven *glo-1(lf)* animals observed displayed the phenomena, as compared with seven of seven in wild-type animals as previously described (Fig. 2H), suggesting that the flashing autofluorescent granules are lysosome-related organelles.

Discussion

Some lysosome-related organelles in the worm intestine exhibit dynamic flashing autofluorescence

In the process of establishing a baseline for fluorescence dynamics in ex vivo intestines, we characterize an intriguing dynamic of lysosome-related organelles. When provided with food, some of the lysosome-related organelles in intestinal cells underwent a rapid change in fluorescence intensities. We observed two distinctive fluorescence dynamics in green and red fluorescence. The dynamic of the green fluorescence is characterized by a sharp and rapid increase in intensity that diffuses into the surrounding area, followed by a rapid decrease and dissipation of the autofluorescence. On the other hand, the dynamic of the red fluorescence is only that of decreases in intensity (Fig. 1). The green and red fluorescence dynamic combination coincidentally resemble the predicted outcome of our original experiment, in which a green pH-sensitive encoded vesicle release

reporter is paired with a red non-pH-sensitive control. The very rare occurrence of the event under conditions without food being present initially misled us as to the source of the fluorescence. Only after the discovery of the effect of food presence did we realize what we were studying was likely a pair of naturally occurring worm fluorophores with an intriguing dynamic.

The gut granule flashing phenomena may be part of a metabolic or signaling process

In the worm intestine, gut granules coexist with more conventional lysosomes (Campbell & Fares, 2010; Kostich et al., 2000; Morris et al., 2018), and although prevailing and distinctive (Chitwood & Chitwood, 1950; Clokey & Jacobson, 1986; Hermann et al., 2005) are not thought to be the major site of intracellular digestion as with lysosome-related organelles in many other spices (Delevoye, Marks, & Raposo, 2019). In *C. elegans*, gut granules have been shown to have both metabolic and signaling functions. The lysosome-related organelles are a site for fat and cholesterol storage (Lee et al., 2015; Schroeder et al., 2007) as well as functioning both as a storage and a sequestering site for micronutrient metals (Chun et al., 2017; Roh et al., 2012). Lysosome-related organelles are also the site of biosynthesis for signaling molecules such as ascarosides (Le et al., 2020). Other than being static sites of storage and metabolic processes, gut granules have been shown to undergo structural and morphological changes responding to changes in dietary conditions. For example, in response to high dietary zinc, gut granules are remodeled from the typical round sphere to bilobed granules with asymmetrical distribution of both internal content and membrane proteins (Roh et al., 2012). The mechanism of such a structural rearrangement remains largely uncharacterized.

The gut granule flashing phenomena were highly associated with the immediate presence of food (Fig. 2). This observation implies that the phenomena could be a part of or a consequence of a

metabolic or signaling process in food intake. One possibility is that this phenomenon is associated with a vesicle content release of the gut granules, and the fluorophores or the content that it is released with plays metabolic or signaling roles in food uptake. Another possibility is that the phenomenon is associated with the breakdown of gut granules, either as part of a physiological process or as a result of our *ex-vivo* experimental conditions. Two reasons argue that the second possibility is less likely than the first. First of all, we have, on rare instances, observed similar events in intact worms, albeit we have not been able to record such events. We have also observed multiple flashing events in some of the granules. Secondly, the phenomenon is visually different from that of the visualized fluorescently labeled gut granules disruption in osmotic sensitive mutants under hypotonic shock (Luke et al., 2007), although there is some similarity in the diffusion of the fluorescence. Whatever the case, it would be interesting to know the identity of the at least two fluorophores involved.

C. elegans are long known to be autofluorescent (Babu, 1974), with most of the autofluorescence from the gut granules (Clokey & Jacobson, 1986). Particular interest has been paid to the increasing level of autofluorescence as the worms age (Clokey & Jacobson, 1986; Davis, Anderson, & Dusenbery, 1982; Forge & Macguidwin, 1989; Klass, 1977; Pincus, Mazer, & Slack, 2016). However, the fluorophores responsible for gut granule autofluorescence remain largely undefined. One of the fluorophores emitting blue fluorescence has been identified as anthranilic acid (Babu, 1974; Coburn et al., 2013), and changes in the blue fluorescence near the death of the animals (death fluorescence, or DF) has been described (Coburn et al., 2013; Pincus et al., 2016). Although both green and red fluorescence also increase with age and green fluorescence intensifies near the death of the animals (Coburn et al., 2013; Pincus et al., 2016), the patterns of the fluorescence changes are different, and they are also likely emitted by different fluorophores. It is also important to note that

the fluorescence dynamic of DF is also distinct from the phenomenon that we are describing in this research, both spatially and temporally.

A major caveat of this study is its *ex-vivo* nature. One could argue that the fluorescence dynamic we observed may not be physiological. It is important to stress, however, that besides the fact that we have been able to observe the phenomenon in live worms on a few occasions, the phenomenon is dependent upon a potential environmental cue- the presence of food; and is genetically dependent on the gene *glo-1*. It is also worth noting that conditions such as oxidative stress does not appear to increase autofluorescence in *C. elegans* (Pincus et al., 2016). Regardless, even if the phenomenon is not itself naturally occurring, it is a beautiful experimental phenotype that could also be informative.

Further understanding of the phenomenon would likely require the characterization of the green and red fluorophores. It is unclear how to best identify these fluorophores, although we would predict that the green fluorophores emit stronger fluorescence under low pH conditions, while the red fluorophores are likely pH neutral. Nonetheless, we described a visually spectacular fluorescence dynamic phenomenon that involves a type of lysosome-related organelles known as gut granules in nematode intestines. It is possible that what we observed is part of a common cellular process but only visualized through the strong autofluorescence of the fluorophores. If that is the case, the gut granules of *C. elegans*, with its naturally occurring fluorophores, may be a potential platform for the understanding of lysosome-related organelles as well as cellular vesicle membrane dynamics.

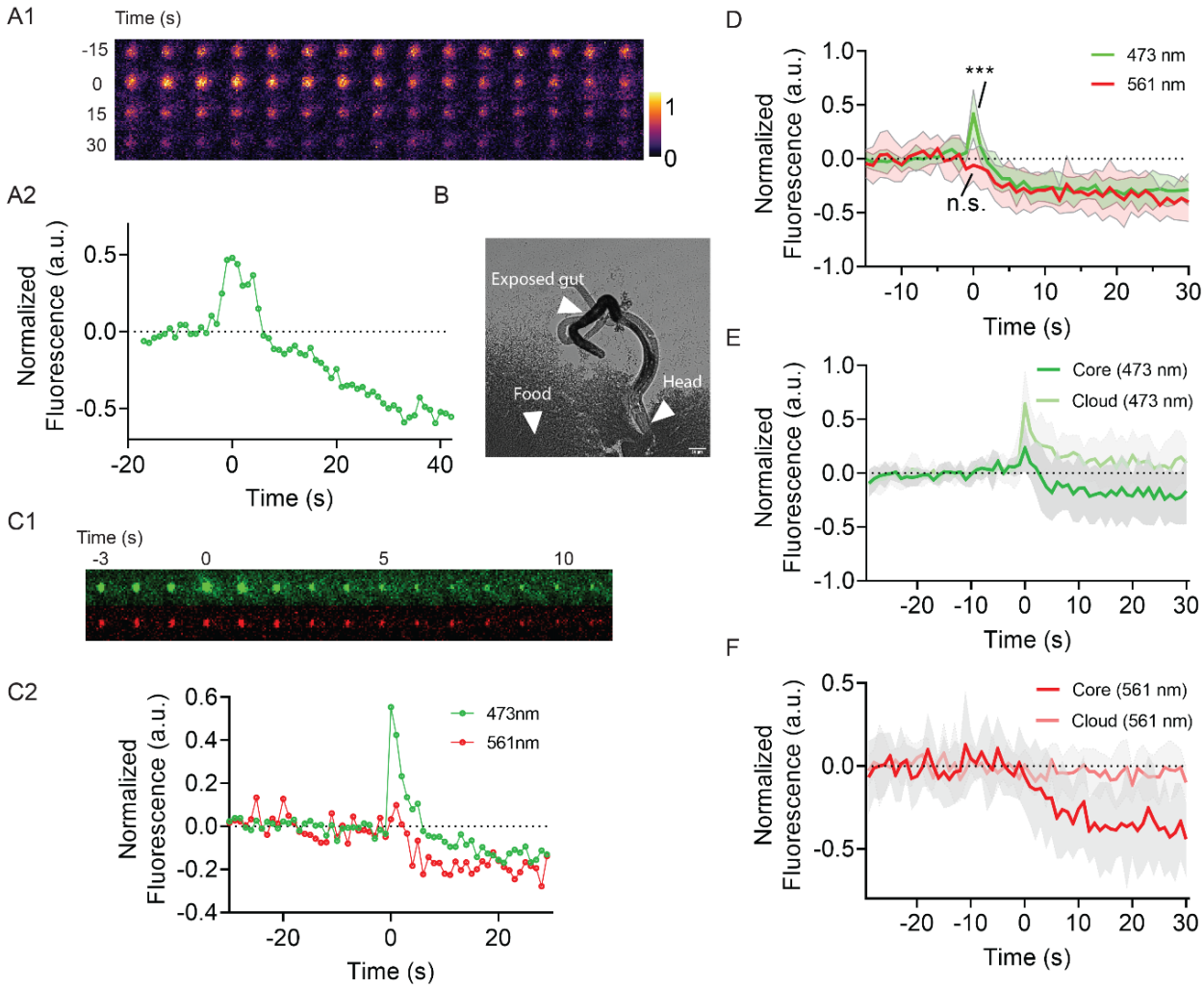

Figure 1: The dynamics of gut granule dissipation.

(A) The green fluorescence in the granule increases and falls sharply. Representative example of changes in green fluorescence intensity during gut granule dissipation. (A1) A 1-minute pseudo-color time series of a gut granule dissipation event. Imaging rate: 1Hz. The time axis is zeroed at the dissipation onset (see Methods). (A2) Normalized green fluorescent intensity plot of (A1). (B) An example of the ex-vivo experimental setting. L4 stage nematodes were carefully incised near the anus to expose the gut. In the "with food" conditions, nematodes were positioned to embed their heads in food. (C-D) The green fluorescence in the granule increases and falls sharply, while the red lack the initial sharp increase. (C) A representative example of two-color time-lapse imaging (C1) and normalized quantifications (C2). The fluorescence intensity is normalized by the baseline fluorescence calculated as the mean of fluorescence in the ROIs prior to the dissipation onset. (D) The average fluorescence intensity of all recorded dissipations in one sample. (E-F) Gut granule flashes during dissipation. Two-color imaging of all recorded gut granule dissipation events in a representative sample. (E-F) The granular area ("core"), as well as the surrounding ring area that presents diffusion of fluorescence ("cloud"), were measured separately in both 473nm (E) and 561nm (F) illumination. (E). The intensity increase in green fluorescence is not only limited to the original "core" area but also to the surrounding areas "cloud ."(F) No intensity increase was observed with the red fluorescence, neither in the "core" nor the "cloud ." Raw images for analysis were

identical to (D), except a longer pre-onset timeframe was selected for normalization. In (D-F), pooled values are presented as mean ± s.d (N=11 in D, N=8 in E and F). The time axis is zeroed at the dissipation onset. Scale bar, 50 μm.

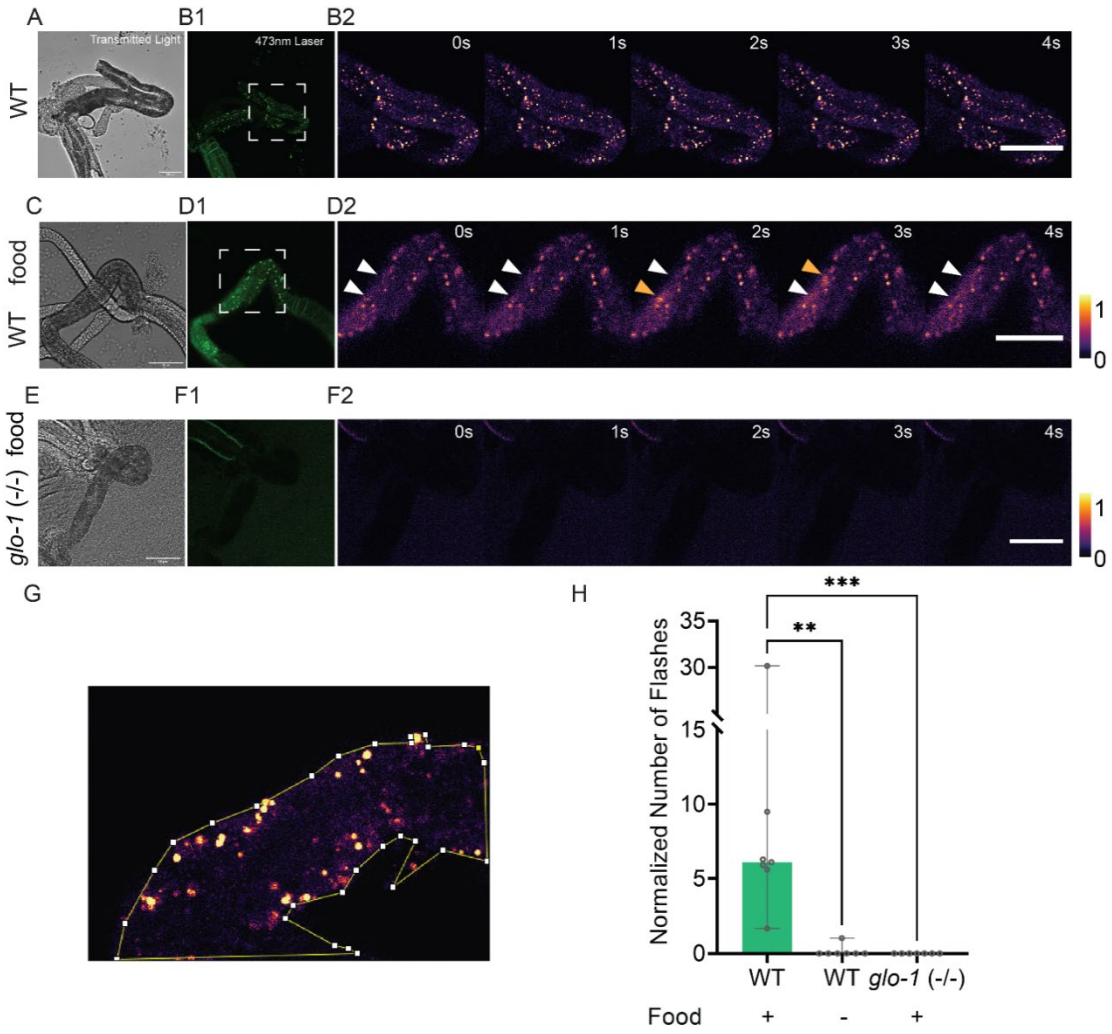

Figure 2: The gut granule dissipation phenomena are dependent on the presence of food.

The field of view was illuminated and recorded with transmitted light (A, C, E), epifluorescence (B1, D1, F1), and 473nm laser illumination (B2, D2, F2). In (B2, D2, F2) 5-second clips of time-series with 473nm laser illumination were pseudo-colored and shown. (A-B) In wild-type worms not provided with food on slide, the phenomena were rarely observed. (C-D) In wild-type worms provided with food on slide, the occurrences of phenomena were increased dramatically. Orange arrows in (D2) indicate the onset of gut granule dissipation events. White arrows point to the same region of interest before and after onset. (E-F) There is no detection of events in *glo-1(lf)* worm even with the presence of food on slide. (G-H) Gut granule dissipation events were manually identified and scored. To normalize the number of events for comparison, the counts for each sample were divided by (1) the area of exposed intestine within the field of view as shown in (G) and (2) by the length of time series (details in Materials and Methods). (H) Normalized data from all conditions were plotted (N=6-7), and each group was compared with the WT + food group (**P<0.01, ***P<0.001, Mann-Whitney *U* test). Scale bar, 50 μm.

Methods

Nematode strains maintenance and general methods.

The culture and maintenance of *C. elegans* w were done similarly to the standard procedure as described in Brenner (1974). Briefly, worms were cultured on Nematode Growth Medium (NGM) dishes with a lawn of *Escherichia coli* strain OP50 at 20°C. The Bristol N2 strain (Brenner, 1974) was used as the wild-type reference strain, and from which the mutant strain was derived. The five times out-crossed *glo-1(zu391 lf)* X (Hermann et al., 2005) mutant strain OJ1347 (Wang et al., 2013) was a gift from Dr. Derek Sieburth of the University of Southern California.

Sample preparation for *ex-vivo* imaging.

L4 stage hermaphrodite worms were transferred to a drop of Iwasaki–Teramoto (I–T) solution (Teramoto & Iwasaki, 2006) [136mMNaCl, 9mMKCl, 1mM $CaCl_2$, 3mM $MgCl_2$, 77mM glucose, and 5mM HEPES (pH 7.4)] and immobilized with 1mM levamisole on a microscopic slide. To expose the intestine for imaging, worms were incised with a pair of 30G 5/8" needles (PrecisionGlide, BD, Franklin Lakes, NJ) near the anus. For experiments with food added on the slide, a glob of OP50 collected by scrapping the lawn off an NGM plate using a cell scraper was transferred into the droplet via the platinum wire worm pick. An insulation spacer was drawn using a PAP pen (RPI, #195506) around the solution droplet, and a piece of cover-glass was mounted atop subsequently.

Microscopy

Confocal time series were acquired using a Fluoview FV3000 Confocal laser scanning biological microscope (Olympus) with a 60×, 1.30 N.A. silicone oil objective (Olympus). Frame rate was

calibrated to 1Hz by adjusting the size of the imaging window and the line averaging multiplier. 5-min time lapse imaging was acquired for each sample. All image processing and analyses were done using ImageJ (National Institute of Health). The transmitted light channel was illuminated simultaneously with the imaging laser (473nm) for positional imaging. Panel A1 in Figures 1, as well as Panels B2, D2, F2 and G in Figure 2, were pseudo-colored with mpl-inferno LUT in FIJI.

Imaging data processing

ROIs of granules were manually selected in FIJI for all data. For Figure 2(G-H), ROIs of peri-granule "cloud" were defined based on the identification of fluorescent pattern of dissipation events. The time series data were zeroed at the flashing onsets of each granule and pooled into metadata.

ROI selection: ROIs were defined based on visual identification of granules in the intestine region, fluorescence normalization baseline was set accordingly as the average of pre-dissipation period. Standard deviation envelopes were visualized in the time series. For Figure 2(H), the number of gut granule dissipation events was normalized as per minute *10-4 μm^2 of the intestinal surface area from single optical sections, which are manually delineated (Figure 2(G)). Nonparametric Mann-Whitney U test was used for comparison between WT food vs. no-food, and WT food vs. *glo-1(lf)*.

Data and Statistical analysis

Data were plotted as mean± s.d, except in Figure 2(H), as raw data failed to passed all normality tests (Kolmogorov-Smirnov test, Shapiro-Wilk test, D'Agostino & Pearson test). Data in Figure 2(H) were plotted as median ± 95% CI instead. All data analysis was performed with Graphpad Prism 9 and Microsoft Excel.

References

Babu, P. (1974). Biochemical Genetics of Coenorhabditis-Elegans. *Molecular and General Genetics*, *135*(1), 39-44. https://doi.org/10.1007/Bf00433899

Brenner, S. (1974). The genetics of Caenorhabditis elegans. *Genetics*, *77*(1), 71-94.

Campbell, E. M., & Fares, H. (2010). Roles of CUP-5, the Caenorhabditis elegans orthologue of human TRPML1, in lysosome and gut granule biogenesis. *BMC Cell Biol*, *11*, 40. https://doi.org/10.1186/1471-2121-11-40

Chitwood, B., & Chitwood, M. (1950). Introduction to nematology (reprinted 1974). In: Baltimore: University Park Press.

Chun, H., Sharma, A. K., Lee, J., Chan, J., Jia, S., & Kim, B. E. (2017). The Intestinal Copper Exporter CUA-1 Is Required for Systemic Copper Homeostasis in Caenorhabditis elegans. *Journal of Biological Chemistry*, *292*(1), 1-14. https://doi.org/10.1074/jbc.M116.760876

Clokey, G. V., & Jacobson, L. A. (1986). The autofluorescent "lipofuscin granules" in the intestinal cells of Caenorhabditis elegans are secondary lysosomes. *Mech Ageing Dev*, *35*(1), 79-94. https://doi.org/10.1016/0047-6374(86)90068-0

Coburn, C., Allman, E., Mahanti, P., Benedetto, A., Cabreiro, F., Pincus, Z., Matthijssens, F., Araiz, C., Mandel, A., Vlachos, M., Edwards, S. A., Fischer, G., Davidson, A., Pryor, R. E., Stevens, A., Slack, F. J., Tavernarakis, N., Braeckman, B. P., Schroeder, F. C., . . . Gems, D. (2013). Anthranilate fluorescence marks a calcium-propagated necrotic wave that promotes organismal death in C. elegans. *PLoS Biol*, *11*(7), e1001613. https://doi.org/10.1371/journal.pbio.1001613

Dal Santo, P., Logan, M. A., Chisholm, A. D., & Jorgensen, E. M. (1999). The inositol trisphosphate receptor regulates a 50-second behavioral rhythm in C. elegans. *Cell*, *98*(6), 757-767. https://doi.org/10.1016/s0092-8674(00)81510-x

Davis, B. O., Jr., Anderson, G. L., & Dusenbery, D. B. (1982). Total luminescence spectroscopy of fluorescence changes during aging in Caenorhabditis elegans. *Biochemistry*, *21*(17), 4089-4095. https://doi.org/10.1021/bi00260a027

Davis, P., Zarowiecki, M., Arnaboldi, V., Becerra, A., Cain, S., Chan, J., Chen, W. J., Cho, J., da Veiga Beltrame, E., Diamantakis, S., Gao, S., Grigoriadis, D., Grove, C. A., Harris, T. W., Kishore, R., Le, T., Lee, R. Y. N., Luypaert, M., Muller, H. M., . . . Sternberg, P. W. (2022). WormBase in 2022-data, processes, and tools for analyzing Caenorhabditis elegans. *Genetics*. https://doi.org/10.1093/genetics/iyac003

Delevoye, C., Marks, M. S., & Raposo, G. (2019). Lysosome-related organelles as functional adaptations of the endolysosomal system. *Curr Opin Cell Biol*, *59*, 147-158. https://doi.org/10.1016/j.ceb.2019.05.003

Forge, T. A., & Macguidwin, A. E. (1989). Nematode autofluorescence and its use as an indicator of viability. *J Nematol*, *21*(3), 399-403.

Hermann, G. J., Schroeder, L. K., Hieb, C. A., Kershner, A. M., Rabbitts, B. M., Fonarev, P., Grant, B. D., & Priess, J. R. (2005). Genetic analysis of lysosomal trafficking in Caenorhabditis elegans. *Mol Biol Cell*, *16*(7), 3273-3288. https://doi.org/10.1091/mbc.e05-01-0060

Klass, M. R. (1977). Aging in the nematode Caenorhabditis elegans: major biological and environmental factors influencing life span. *Mech Ageing Dev*, *6*(6), 413-429. https://doi.org/10.1016/0047-6374(77)90043-4

Kostich, M., Fire, A., & Fambrough, D. M. (2000). Identification and molecular-genetic characterization of a LAMP/CD68-like protein from Caenorhabditis elegans. *J Cell Sci*, *113 (Pt 14)*, 2595-2606. https://doi.org/10.1242/jcs.113.14.2595

Laufer, J. S., Bazzicalupo, P., & Wood, W. B. (1980). Segregation of developmental potential in early embryos of Caenorhabditis elegans. *Cell*, *19*(3), 569-577. https://doi.org/10.1016/s0092-8674(80)80033-x

Le, H. H., Wrobel, C. J., Cohen, S. M., Yu, J., Park, H., Helf, M. J., Curtis, B. J., Kruempel, J. C., Rodrigues, P. R., Hu, P. J., Sternberg, P. W., & Schroeder, F. C. (2020). Modular metabolite assembly in Caenorhabditis elegans depends on carboxylesterases and formation of lysosome-related organelles. *Elife*, *9*. https://doi.org/10.7554/eLife.61886

Lee, H. J., Zhang, W., Zhang, D., Yang, Y., Liu, B., Barker, E. L., Buhman, K. K., Slipchenko, L. V., Dai, M., & Cheng, J. X. (2015). Assessing cholesterol storage in live cells and C. elegans by stimulated Raman scattering imaging of phenyl-Diyne cholesterol. *Sci Rep*, *5*, 7930. https://doi.org/10.1038/srep07930

Luke, C. J., Pak, S. C., Askew, Y. S., Naviglia, T. L., Askew, D. J., Nobar, S. M., Vetica, A. C., Long, O. S., Watkins, S. C., Stolz, D. B., Barstead, R. J., Moulder, G. L., Bromme, D., & Silverman, G. A. (2007). An intracellular serpin regulates necrosis by inhibiting the induction and sequelae of lysosomal injury. *Cell*, *130*(6), 1108-1119. https://doi.org/10.1016/j.cell.2007.07.013

Morris, C., Foster, O. K., Handa, S., Peloza, K., Voss, L., Somhegyi, H., Jian, Y., Vo, M. V., Harp, M., Rambo, F. M., Yang, C., & Hermann, G. J. (2018). Function and regulation of the Caenorhabditis elegans Rab32 family member GLO-1 in lysosome-related organelle biogenesis. *PLoS Genet*, *14*(11), e1007772. https://doi.org/10.1371/journal.pgen.1007772

Pincus, Z., Mazer, T. C., & Slack, F. J. (2016). Autofluorescence as a measure of senescence in C. elegans: look to red, not blue or green. *Aging (Albany NY)*, *8*(5), 889-898. https://doi.org/10.18632/aging.100936

Roh, H. C., Collier, S., Guthrie, J., Robertson, J. D., & Kornfeld, K. (2012). Lysosome-related organelles in intestinal cells are a zinc storage site in C. elegans. *Cell Metab*, *15*(1), 88-99. https://doi.org/10.1016/j.cmet.2011.12.003

Schroeder, L. K., Kremer, S., Kramer, M. J., Currie, E., Kwan, E., Watts, J. L., Lawrenson, A. L., & Hermann, G. J. (2007). Function of the Caenorhabditis elegans ABC transporter PGP-2 in the biogenesis of a lysosome-related fat storage organelle. *Mol Biol Cell*, *18*(3), 995-1008. https://doi.org/10.1091/mbc.e06-08-0685

Teramoto, T., & Iwasaki, K. (2006). Intestinal calcium waves coordinate a behavioral motor program in C. elegans. *Cell Calcium*, *40*(3), 319-327. https://doi.org/10.1016/j.ceca.2006.04.009

Thomas, J. H. (1990). Genetic analysis of defecation in Caenorhabditis elegans. *Genetics*, *124*(4), 855-872.

Wang, H., Girskis, K., Janssen, T., Chan, J. P., Dasgupta, K., Knowles, J. A., Schoofs, L., & Sieburth, D. (2013). Neuropeptide secreted from a pacemaker activates neurons to control a rhythmic behavior. *Curr Biol*, *23*(9), 746-754. https://doi.org/10.1016/j.cub.2013.03.049